The effect of pH adjustment on the properties and pressure filtration characteristics of bauxite residue slurries

Kinnarinen Teemu, Theliander Hans, Häkkinen Antti, Mattsson Tuve

DOI: 10.1016/j.seppur.2018.11.039

The effect of pH adjustment on the properties and pressure filtration characteristics of bauxite residue slurries

Teemu Kinnarinen[a*], Hans Theliander[b], Antti Häkkinen[a], Tuve Mattsson[b]

[a]LUT School of Engineering Science, Lappeenranta University of Technology,
Skinnarilankatu 34, FI-53850, Lappeenranta, Finland
[b]Department of Chemistry and Chemical Engineering,
Chalmers University of Technology, SE-412 96 Gothenburg, Sweden

[*]Corresponding author: Teemu Kinnarinen (teemu.kinnarinen@lut.fi)

Abstract

The influence of the slurry pH on the characteristics of a topical unit operation, pressure filtration of bauxite residue slurries, was investigated in this experimental study. The primary aim of pH adjustment is to precipitate aluminate off from the liquid phase and to facilitate safe disposal of the residue. In the investigated cases, pH adjustment was performed with hydrochloric acid. The experiments were carried out by using two types of pressure filters, a Nutsche filter unit used for the acquisition of average filtration data, and a piston press used for measuring local cake characteristics. The Nutsche filter was used to separate the bauxite residue slurry with a pH of 13.3 and 11.0 at three different filtration pressures (300, 450 and 600 kPa), while the piston press was operated under a constant filtration pressure of 1200 kPa and with a wider pH range (13.3, 11.0 and 7.0). The average particle/agglomerate size increased as the pH was reduced, however, the width of particle size distribution increased somewhat as well when the pH was adjusted to 7.0. Based on the average cake properties, it could be concluded that the specific cake resistance and cake compressibility index increased, while cake solidosity decreased as the slurry pH was reduced from 13.3 to 11.0. The final average solidosity (at 300 kPa) decreased from 0.43 to 0.31 when the pH was adjusted from 13.3 to 11.0. The local filtration properties also showed that the cake became more compressible and the structure of the cake more porous as a consequence of pH reduction. The local hydrostatic pressure measurements indicated that the expression rate of the cakes was decreased for filter cakes formed from a slurry with a lower pH level (pH 11 and 7 compared to a pH of 13.3).

1. Introduction

Global alumina production is facing a huge challenge due to the large quantities of waste generated by the Bayer process. Digestion of bauxite ore at high temperatures and strongly alkaline conditions yields a concentrated aluminate solution for further processing for alumina recovery, while the non-digested solid fraction, i.e. bauxite residue, is washed and disposed of. The annual production of bauxite residues has been estimated to be approximately 120-150 million tonnes [1,2], the global inventory of bauxite residues being as high as about 3 billion tonnes [3,4]. Therefore, it is of great importance to ensure safe and efficient utilization or disposal of these residues. Due to the large amounts of bauxite residue, the potential to use it for large-scale applications is generally regarded as significant, although commercial utilization is still scarce [5,6]. In the literature, the most commonly discussed methods for utilization include production of

various construction materials [7], soil amendment, ceramics, various adsorbents [8-10], coagulants [11], and pigments [12]. The recovery of metals by leaching [13-15], especially rare earth elements [5,16], possibly after recovery of iron by smelting [17,18] or reductive roasting [19], seems to be an option worth considering as well.

Bauxite residues are strongly alkaline and have a high pH, ranging from approximately 10 to over 13 [20,21], depending on the applied treatment sequence. In order to recover aluminate and alkali, countercurrent washing of bauxite residue is carried out in a series of washing decanters, from where the final thickened underflow stream may be pumped to filters for further separation, or directly to the disposal area. Disposal after thickening, at a total solid content of < 55 %, is referred to as dry stacking, and disposal after filtration, at a solid content of approximately 60-75 %, is referred to as dry cake disposal. Dry cake disposal after filtration with filter presses is becoming more common due to its economic and environmental benefits, and it is currently in use at many refineries e.g. in Brazil, Greece, Turkey, and China [22]. The most commonly used filters for the purpose of dry cake disposal include rotary vacuum filters, rotary hyperbaric filters and various filter presses. The highest dryness of filter cake is obtainable with filter presses [23], due to the possibility to use high pressure differences in the filtration, cake squeezing and air dewatering stages. A compact filter cake with a low caustic content (pH = 10-12) is better suited for safe disposal and utilization of the residue as raw material for various purposes [3]. Reduction of the pH by using seawater, CO_2, SO_2 or mineral acids [24,25] has been observed to help mitigate the harmful effects of bauxite residues on living organisms [26,27]. In addition to the harmful impacts caused by alkalinity, some soluble metals ions, such as vanadium, may pose a cause for concern [28]. To avoid leaching of metals out of the solids, as reported e.g. in [29], the pH should not be reduced excessively to the acidic side. It has been observed in previous studies [30-32] that the bauxite residue solids have a high buffering capacity. This is a consequence of the composition of the solid phase, where the readily soluble desilication products, such as Bayer sodalite, play a major role [3,30,33].

The filtration properties of a slurry are very difficult to predict from particle and slurry properties alone, and in most cases they must be studied experimentally by performing filtration tests. The modeling of filtration behavior based on test filtration data is often performed by using the classical filtration equation [34] based on flow through porous beds [35], where only average properties of the forming filter cake are considered. This approach is easy to use and works well in various applications. However, for cases where the filter cake displays compressible behavior, i.e. the cake structure and thus the flow resistance varies within the cake, according to the applied pressure, also local properties need to be considered to describe the filtration behavior of the slurry accurately. Minerals often form cakes with low compressibility [36], but for cases where a change in the slurry conditions (e.g. pH or ionic strength) has induced increased agglomeration, a considerable degree of compressibility has been found for mineral materials as well [37,38]. In these cases, also local filtration properties, such as local cake solidosity and hydrostatic pressure profiles need to be considered and studied to be able to describe the filtration process accurately.

Previous studies regarding the pH reduction of bauxite residue slurries have focused on describing the chemistry of neutralization in close detail [6,21,31,32], but the impacts of pH on the solid-liquid separation characteristics of these residues have not been studied, although the need for understanding the resulting changes in the dewatering and compression properties has been

recognized e.g. by Kirwan et al. [31]. The aim of this paper is to study how the pH of the bauxite residue slurry affects the average and local pressure filtration properties, and how these changes in filtration behavior are related to changes in the properties of the slurry. The study is of high importance, regarding the current industrial practices in the treatment of bauxite residues.

2. Materials and methods

2.1. Bauxite residue slurries

A primary slurry sample (0.3 m^3) was taken at an alumina refinery from the underflow of the last washing thickener. A sub-sample with a volume of 15 dm^3, taken from the well-agitated primary slurry sample was used in the experiments. For the first series of experiments, part of the slurry sample was ground with a stirred media mill (Vollrath-Salomix, P = 0.75 kW) using glass beads, in order to investigate the influence of particle size reduction on the filtration behavior. The grinding conditions were as follows: grinding time = 30 min, rotation speed = 700 rpm, mass of slurry = 4.0 kg, vessel volume = 5.4 dm^3, mass of beads = 2.0 kg, and diameter of beads = 2.0 mm. A pin stirrer (for details see [39]) was used as the mixing element. Separation of the beads from the slurry after grinding was carried out by pouring the slurry through a 1.4 mm sieve.

The properties of the slurry samples at different pH levels are summarized in Table 1. The density (ρ_{Slurry}) of the slurry was calculated on the basis of the mass and volume of a slurry sample. To determine the total solids (TS) content, the slurry sample was dried in an oven at 105 °C. The concentration of total dissolved solids (TDS) in the liquid phase of the slurry was determined by drying a sample of centrifuged supernatant in the oven at 180 °C to total dryness. The total caustic (TC), comprising the free OH^- content and one mol OH^- per mol aluminate present, was determined by using a Metrohm 859 thermometric titrator.

Rheology of the slurries at different solid concentrations and pH was investigated with an Anton Paar Modular Compact Rheometer MCR 302. The particle size distributions of the original, ground and pH-adjusted slurries were measured with a Malvern Mastersizer 3000 laser diffraction analyzer. Particle size distribution measurements were performed on diluted (< 10 wt.%) samples at least five times, the average distributions of the trials were calculated, and are presented together with the rheological measurements in the "Results and discussion" section of this paper. The elemental composition of the dissolved solids in the liquid phase of the bauxite residue slurry where investigated as well. The analysis was performed with SEM-EDS, using a Hitachi SU 3500 scanning electron microscope on dried samples (evaporated at 180 °C) of clear supernatant, which was separated from the slurry by centrifugation. These results are also reported in the "Results and discussion" section.

The density of the solid phase in the slurry at pH 11 (ρ_s = 2850 kg m^{-3}) and pH 13 (ρ_s = 2940 kg m^{-3}) was measured by a gas pychnometer (Micrometics AccuPyc II) after drying the slurry sample at 105 °C. These values were used as estimated solid densities when the average solidosities of the cakes were calculated.

Hydrochloric acid (HCl) was selected to be used as the source of H^+ for the pH reduction of the slurry. The reduction of the slurry pH to 11.0 required a HCl (37 %) dosage of 9.5 w-% in relation to the original slurry weight. Due to the high solid content of the slurry and agglomerating effect of pH reduction, it was necessary to add a small amount of water (9.0 % of the mass of the pH-adjusted slurry) to reduce the viscosity and thus enable slurry feed into the filters. In order to adjust the slurry pH to 7.0, 123 g of 37 % HCl per kg of original slurry was added. The properties presented in Table 1 are the ones obtained after the dilutions were performed.

Table 1. Properties of bauxite residue slurries at pH 13.3, 11.0, and 7.0.

Slurry pH (-)	ρ_{Slurry} (kg m^{-3})	TS* (g kg^{-1})	TDS** (g kg^{-1})	TC as Na_2O*** (g kg^{-1})	D[3,2], original (µm)	D[3,2], ground (µm)
13.3 (As received)	1450	498	124	45	2.16	1.90
11.0 (Reduced)	≈ 1400	446	99	2.2	4.23	3.55
7.0 (Further reduced)	≈ 1400	444	77	≈ 0****	3.58	-

**Total solids with respect to slurry*
***Total dissolved solids with respect to liquid phase*
****Total caustic with respect to liquid phase*
*****Not measured, see [40]*

The main effect of the addition of HCl in the caustic aluminate liquor can be described in a simplified way by the following generalized reaction equations [31,32]:

Aluminate:

$$Al(OH)_4^-(aq) + H^+ \rightarrow Al(OH)_3(s) + H_2O \quad (1)$$

Hydroxide:

$$OH^- + H^+ \rightarrow H_2O \quad (2)$$

Carbonate:

$$CO_3^{2-}(aq) + H^+ \rightarrow HCO_3^- \quad (3)$$

In fact, when HCl is used as the source of H^+, the reactions above also produce sodium chloride, which is highly soluble in the slurry liquor. The reactions presented in Eqs. (1-3) are unable to describe all changes taking place in the slurry, due to the diverse composition of the solid and liquid phases. However, the main solid reaction product formed from the dissolved solids content of the liquid phase is gibbsite $Al(OH)_3$.

The main reactions in the solid phase include dissolution of calcium minerals, for instance tricalcium aluminate, and dissolution/desorption of desilication products, for instance sodalite, according to Eqs. (4) and (5), respectively [31]:

$$Ca_3Al_2(OH)_{12}(s) + 6H^+ \leftrightarrow 3Ca^{2+} + 2Al(OH)_3(s) + 6H_2O \quad (4)$$

$$Na_6Al_6Si_6O_{24} \cdot Na_2CO_3 \cdot yH_2O(s) + 18H_2O + 7H^+ \leftrightarrow 8Na^+ + 6Al(OH)_3(s) + 6Si(OH)_4(s) + HCO_3^- + yH_2O \quad (5)$$

2.2. Filter units

Two different filter units were used in order to study the average and local filtration properties at different pH levels. All experiments were performed at room temperature (21-23 °C). The average filtration properties at pH 13.3 and 11.0 were studied by using a Nutsche filter, while a piston press was used in order to measure the local pressure and solidosity profiles within the filter cakes, as well as the average filtration properties, at pH 13.3, 11.0 and 7.0. Both filter units are depicted in Fig. 1 and described below.

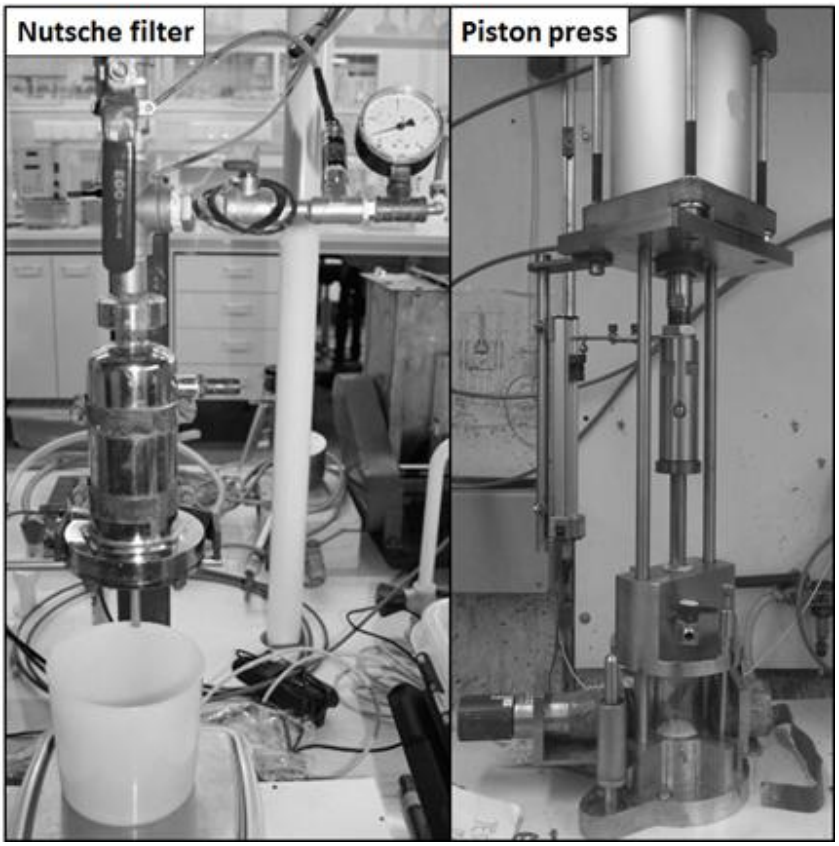

Figure 1. Nutsche filter used in measuring the average filtration properties at pH 13.3 and 11.0, and piston press used in measuring the local filtration properties at pH 13.3, 11.0 and 7.0.

2.2.1. Nutsche filter

The first pressure filter was of the Nutsche type, i.e. the filter chamber was pressurized with compressed gas to create the driving force for filtration. The maximum operating volume of the

filter chamber in this batchwise operated device was 350 cm^3, and the mass of the slurry fed into the filter was 0.250 kg in all experiments. The filtration area was 0.002 m^2, and the applied filtration pressures (Δp) were 300, 450 and 600 kPa. With this filter, filtration experiments were performed at pH 13.3 (without HCl addition) and at pH 11.0, using both the original and ground slurries.

The filter medium in the Nutsche filter was a cellulosic disc (model T1000, Pall Corporation, Germany), which was allowed to soak in water for at least one hour before being installed on the bottom of the filter chamber. During each experiment, the filtrate weight and filtration pressure were measured once a second. The average specific cake resistance, as well as the average solidosity of the filter cake at the end of the filtration were calculated based on the filtrate, cake dimensions, and the wet and dry weight of the cake.

2.2.2. Piston press

The instrumentation of the piston press enabled the study of the local solidosity of the filter cake and the local hydrostatic pressure at various heights in the cake during filtration. The piston press was powered by a pneumatic pressure cylinder (Bosch Rexroth AB, cyl167/200/130), and could produce a maximum filtration pressure of 6 MPa. Measurement of the piston position was performed by using a Temposonics EP-V-0200M-D06-1-V0 position sensor. The total height and diameter of the cylindrical filter cell were 17.5 and 6 cm, respectively, and the lower part consisted of a Plexiglas cylinder (height = 11.5 cm), which enabled both a low γ-attenuation and visual observation. On the bottom of the cell, a perforated plate was used as a support for the filter medium (Munktell grade 5 filter paper). Local hydrostatic pressures were measured at several distances, 12, 9, 7, 5, 3, 2, 1, 0.5 mm, from the filter medium by using eight capillary tubes mounted through the filter medium. Each capillary had an aperture close to the top of the tube, perpendicular to the filtrate flow, to enable pressure measurements; a pointed cap on the top of the tube minimized flow disturbances. Blocking of capillaries could be readily detected from the recorded pressure data. In these studies, blocking was observed at the two lowest positions, and thus the data of these two positions is not reported in this work. The filtrate exiting through the bottom of the cell was collected and weighed on a scale (Mettler Toledo SB 32000). The piston position, filtrate weight and local hydrostatic pressures were recorded every two seconds.

Local solidosity at a selected position, 12 mm from the filter medium, was studied during the filtrations by using a γ-attenuation method. For this study, a collimated ^{241}Am γ-source (10^9 Bq) was used in tandem with a detector, both being mounted on a movable rack.

To enable the investigation of a thin slice of the forming filter cake, both the γ-source and the detector were well shielded, with the exception of a horizontal slit; 24 mm wide and 3 mm high at the source, and 24 mm wide and 1 mm high at the detector. Johansson and Theliander [41] have described the apparatus in detail.

2.3. Summary of experimental work performed with different slurries

Table 2 summarizes the main part of the experimental work with different bauxite residue slurries at various conditions.

Table 2. Summary of experiments performed with bauxite residue slurries.

Measurement	Equipment	Slurry type	Slurry pH	Conditions
PSD of solids	Malvern Mastersizer 3000 laser diffraction analyzer	Original	13.3, 12.9, 12.6, 12.1, 11.0, 10.0, 7.0	Ambient T (≈ 22 °C) and p
		Ground	13.3, 11.0	Ambient T and p
Slurry rheology	Anton Paar Modular Compact Rheometer MCR 302	Original and Ground	13.3, 11.0	Ambient T and p, TS = 49.8, 45.0, 41.0 wt.%
Average filtration properties	Nutsche pressure filter, A = 0.002 m^2	Original and Ground	13.3, 11.0	Ambient T, Δp = 300, 450, 600 kPa, TS = 49.8, 44.6, 44.4 wt.%
Local and average filtration properties	Piston press, A = 0.0028m^2	Original	13.3, 11.0, 7.0	Ambient T, Δp = 1200 kPa, TS = 49.8, 44.6, 44.4 wt.%

3. Evaluation of experimental data

3.1. Average cake properties

The average cake properties were evaluated by using the filtration data and cake characteristics obtained by the Nutsche filter and the piston press. The average solidosities Φ_{av} of the filter cakes were calculated from Eq. (6):

$$\Phi_{av} = \frac{V_{ss}}{V_c} \tag{6}$$

where V_{ss} is the volume of suspended solids, i.e. the remainder of $V_{total\ solids}$ - $V_{dissolved\ solids}$ in the overall cake, and V_c is the total volume of the cake.

The average porosity of the cake was defined as the volumetric fraction of void in the cake, and can be related to the average solidosity from Eq. (6):

$$\varepsilon_{av} = 1 - \Phi_{av} \tag{7}$$

The classical filtration equation [34] enables the calculation of average specific cake resistance α_{av} from experimental data according to Eq. (8):

$$\frac{dt}{dV} = \alpha_{av}\mu c\frac{V}{A^2\Delta p} + \frac{\mu R_m}{A\Delta p} \tag{8}$$

where t is time, V is the volume of the filtrate, α_{av} is the average specific filtration resistance (defined according to Eq. (9)), μ is the viscosity of the filtrate, c is the mass of solids per unit filtrate volume, R_m it the resistance of the filter medium, and A is the filtration area.

$$\frac{1}{\alpha_{av}} \equiv \frac{1}{p_c}\int_0^{p_c}\frac{1}{\alpha}\,dp_s \tag{9}$$

where p_c denotes the pressure drop over the filter cake and p_s is the local solid pressure.

For materials that form an incompressible to slightly compressible filter cake, Eq. (8) can be used to determine the average specific filtration resistance, for this case a plot of dt/dV against V will yield a line with a slope proportional to α_{av}.

The cake compressibility index N was approximated on the basis of average specific cake resistances at different Δp by using a simple empirical correlation [42]:

$$\alpha_{av} = \alpha_1 \Delta p^N \tag{10}$$

where α_1 is the specific cake resistance at unit applied pressure.

3.2. Local cake properties

Based on the measurements of the local hydrostatic pressure, p_L, the local solid pressure, p_s, was calculated according to Eq. (11).

$$0 = dp_l + dp_s \tag{11}$$

The measurement of local solidosity of cakes in the piston press was based on the attenuation of γ-radiation as it passed through the filter cell and the cake. Hence, determination of the local solidosity in a slice of the filter cake could be performed by using the Beer-Lambert law:

$$-\ln\frac{n_\gamma}{n_{\gamma,0}} = \mu_{\gamma,l}d_\gamma + (\mu_{\gamma,s} - \mu_{\gamma,l})d_\gamma\Phi \tag{12}$$

where n_γ is the number of counts for the filter cell with cake, $n_{\gamma,0}$ is the number of counts for an empty cell, $\mu_{\gamma,l}$ and $\mu_{\gamma,s}$ are the attenuation coefficients for the liquid and solid phases, respectively, d_γ is the inner diameter of the filter cell, i.e. the path of the γ-radiation in the cell, and Φ is the local solidosity, i.e. the volumetric fraction of suspended solids in the cake at the position of measurement. This method of measuring local solidosity has been described by Johansson and Theliander [41].

The local specific cake resistance α was calculated by using a combination of a modified Darcy equation and the relationship between permeability and specific filtration resistance. After making some simplifying assumptions, the equation becomes [38]:

$$\alpha = -\frac{1}{v\mu\rho_s\Phi}\frac{dp_L}{dz} \tag{13}$$

where v is the superficial flow velocity of the liquid, μ is the viscosity of the filtrate, ρ_s is the density of the solids, and z is the distance from the filter medium.

The compressibility of the filter cakes at different pH levels was evaluated by using semi-empirical constitutive relationship Eqs. (14) and (15).

$$\alpha = \alpha_0\left(1+\frac{p_s}{p_0}\right)^n \tag{14}$$

$$\Phi = \Phi_0\left(1+\frac{p_s}{p_0}\right)^\beta \tag{15}$$

where α_0, Φ_0, p_0, n and β are parameters.

Calculation of the average specific cake resistance from local data was performed according to Eq. (16), which can be derived from Eqs. (9) and (14).

$$\alpha_{av} = \alpha_0\frac{(1-n)\frac{p_c}{p_0}}{\left(1+\frac{p_c}{p_0}\right)^{1-n}-1} \tag{16}$$

4. Results and discussion

4.1. Effect of pH reduction and grinding on the properties and composition of the slurry

The composition of the dissolved solids in the liquid slurry phase, the particle size distribution of the solids, as well as the rheological properties of the slurry were investigated through different pH/mechanical treatments; the results are presented below.

4.1.1 Composition of the liquid phase

The pH adjustment with HCl had a significant impact on the chemical composition of the liquid phase of the slurry. Table 3 presents the elemental composition of the dissolved solids in the liquid phase of bauxite residue slurry at three different pH levels. It is worth noting that the relative amounts of other elements decreased as a result of increasing the chloride content by HCl addition.

Table 3. Elemental composition of the dissolved solids in the oven-dried liquid phase of bauxite residue slurry at pH 13.3 (starting pH), 11.0 (adjusted with HCl) and 7.0 (adjusted further with HCl) measured by using SEM-EDS.

pH 13.3							
Element	C	O	Na	Al	Si	Cl	K
wt. %	10.5	38.5	43.3	4.6	1.04	1.8	0.34
pH 11							
Element	C	O	Na	Al	Cl	K	
wt. %	6.7	13.6	33.2	2.7	43.7	0.12	
pH 7.0							
Element	C	O	Na	Al	Cl	K	Ca
wt. %	8.7	2.8	31.5	0.22	52.9	0.44	3.5

The main effects of the lowering of the pH can be summarized (and related to the reactions, Eqs. (1-5)) as follows:

- Aluminum (i.e. aluminate) is crystallized off from the liquid phase as the pH is reduced, a significant decrease in both aluminum and oxygen can be seen at a pH reduction from 11 to 7 (Eq. (1)).
- Oxygen, present in e.g. soluble hydroxides at pH 13.3, decreases as gibbsite is formed, or by the neutralization reaction producing water (Eqs. (1-2))
- Calcium starts to dissolve from the solids when the pH is reduced to 7.

Removal of Al from the liquid phase by pH reduction with HCl in a case of bauxite residue leachate neutralization has been reported by Burke et al. [43]. In the case of neutralization with H_2SO_4, formation of gibbsite precipitate as a product of reaction between the aluminate and the acid, has been reported to occur at pH < 8 by Howe et al. [26], while Kirwan et al. [31] have reported gibbsite precipitation with a non-specified source of H^+ to occur mainly above pH 10.

4.1.2 Particle size distribution of solids at different pH levels

The influence of pH reduction on particle size distribution for non-ground and ground slurries were investigated at diluted conditions (lower solid concentration as well as ionic strength) by using laser diffraction (Fig. 2a). For both non-ground and ground samples the particle size shifted towards larger sizes as the pH was reduced, which suggests increased particle agglomeration and possibly also formation of a precipitate in the diluted samples. The pH-dependent changes in the surface properties of bauxite residues have been studied by Liu et al. [44], who report isoelectric points ranging from 6.4 to 8.7.

The grinding with the stirred media mill at pH 13.3 resulted in a slight decrease of the larger particles with a diameter of at least tens of microns. The effect of grinding was generally moderate

compared to the effect of pH. Additionally, when the pH of the ground slurry was reduced to 11.0, the difference between the distribution of ground and non-ground samples decreased. Further addition of HCl to adjust the pH to 7.0 started to dissolve the suspended solids, which may be observed as a slight shift towards a distribution having smaller particles, Fig. 2a.

To investigate the effect of pH on the particle size distribution of the suspended solids further, particle size distributions at smaller incremental pH adjustments were investigated for a non-ground sample (Fig. 2b). A considerable shift in particle size distribution was found to occur between pH 12.9 and 12.6, when monomodal distribution was shifted to a wider bimodal distribution, and the fraction of > 10 µm particles increased considerably. Further reduction of the pH to 11.0 caused a further shift towards coarse particles, although the overall width of the distribution was not increased.

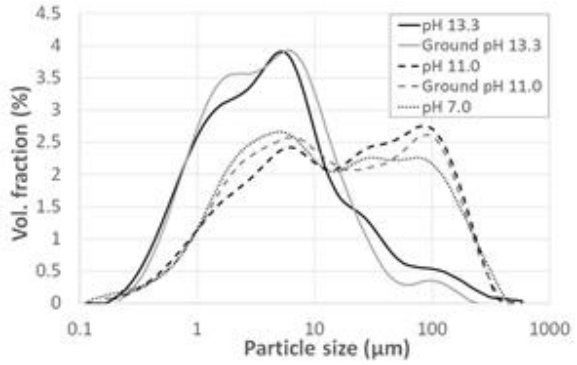

Figure 2a. Particle size distribution for samples of non-ground and ground bauxite residue slurry before and after reducing the pH of the slurries to 11.0.

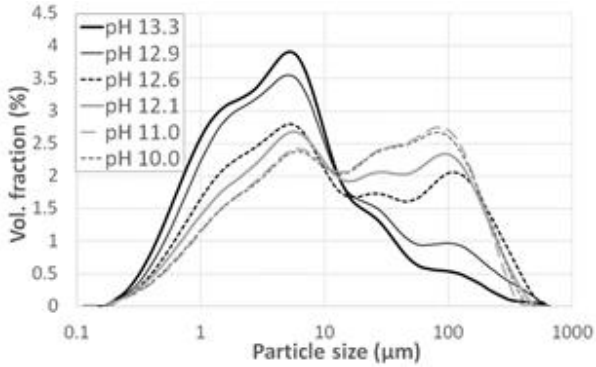

Figure 2b. Particle size distribution for samples from non-ground bauxite residue slurry after different pH adjustments.

4.1.3 Slurry rheology

The changes in the slurry rheology resulting from the mechanical treatment and pH adjustment are illustrated in Fig. 3. The influence of total solids concentration on the rheological properties is also presented. Figs. 3a and 3b present the shear rate dependence of the shear stress and the apparent viscosity for slurries at the original pH (13.3), while the same relationships for the slurries at the adjusted pH (11) are shown in Figs. 3c and 3d. The original solids content of the slurries at pH 13.3 was 49.8 wt.%. Due to the pH adjustment procedure, which inevitably caused the total solids content of the slurry to decrease slightly, the rheological properties at a total solids concentration of 49.8 wt.% were not investigated for the pH-adjusted slurry.

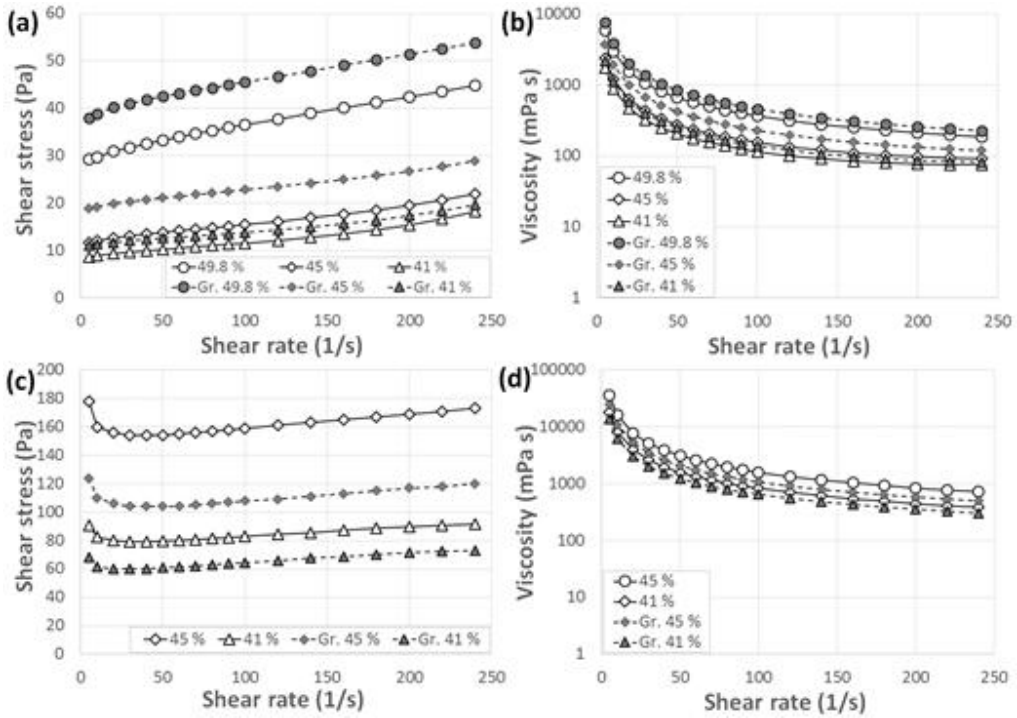

Figure 3. Rheology of the bauxite residue slurry at the original pH 13.3 (a, b) and at pH 11.0 (c,d) when the pH adjustment was done with HCl. Gr. denotes a ground sample.

As Fig. 3 illustrates, the bauxite residue slurries displayed a Bingham plastic behavior at all the investigated conditions. The pH adjustment had a dramatic effect and the slurries at pH 11.0 exhibited a considerably higher yield stress (Figs. 3a and 3c).

The changes in the rheological properties caused by the pH adjustment with HCl can be summarized as three points:

- Adjustment of pH from 13.3 to 11.0 increased the shear stress and the apparent viscosity at a given shear rate greatly. The yield stress increased correspondingly.
- Mechanical treatment seemed to increase the shear stress and the apparent viscosity at the original pH 13.3, but the opposite effect was observed at pH 11.0. The reason for this has not been further investigated in this study.
- Dilution of the slurry improved the ability of the slurries to flow in all cases, reducing the shear stress and the apparent viscosity.

These changes in the rheological properties indicate that the interactions between the species in the system were altered by the pH adjustment.

4.2 Average filtration properties

Filtration experiments with the non-ground and ground bauxite residue slurries were performed at pH 13.3 and 11.0 by using the Nutsche filter at applied filtration pressures of 300, 450, and 600 kPa. The filtration data (d*t/dV* against *V*) of these experiments are presented in Fig. 4. The piston press was utilized in order to evaluate the effect of pH on the filterability of the slurry at an elevated pressure difference of 1200 kPa at three different pH levels (13.3, 11.0, and 7.0). The influence of the slurry pH on the *dt/dV* vs. *V* curves at Δp = 1200 kPa is illustrated in Fig. 5, where also the beginning of the cake consolidation period is shown.

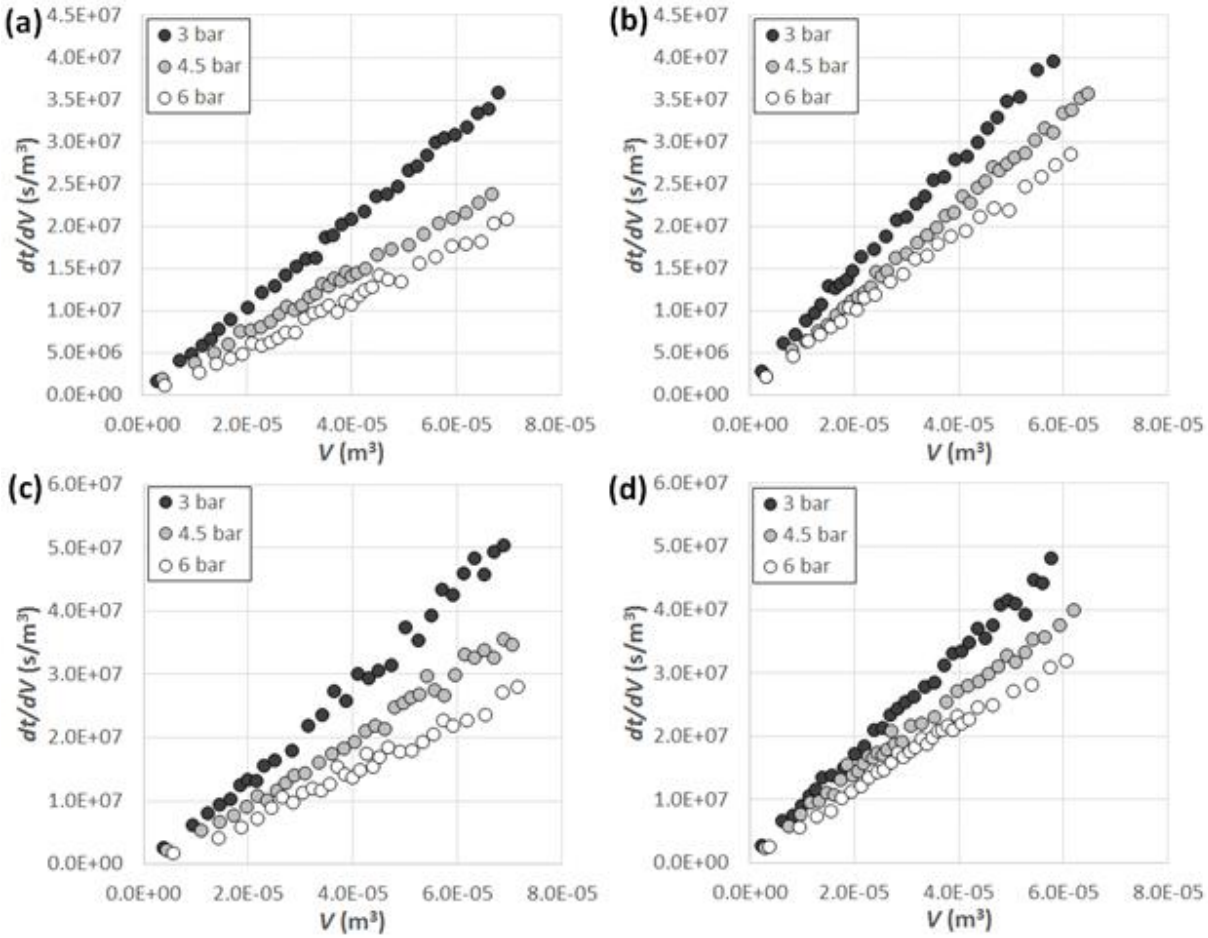

Figure 4. The d*t/dV* vs. *V* plots for the original bauxite residue slurry at pH 13.3 and 11.0 (a,b), and corresponding plots for the ground bauxite residue slurry at pH 13.3 and 11.0 (c,d).

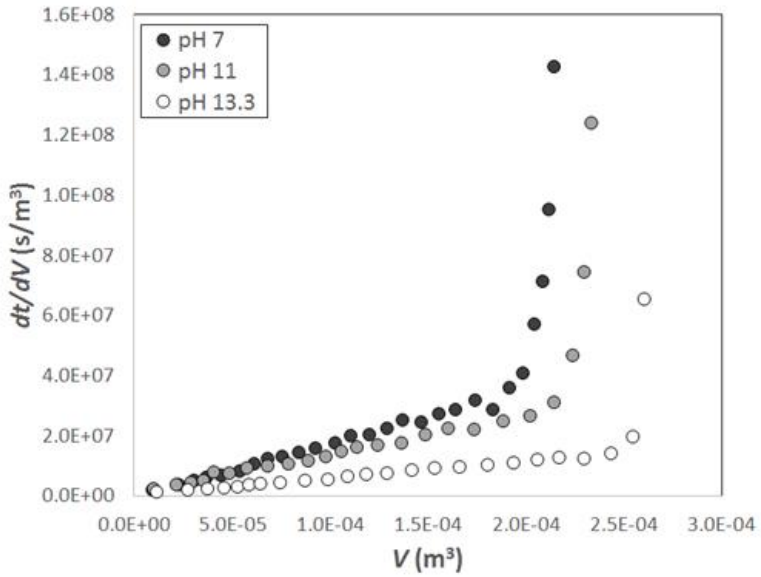

Figure 5. Filtration results obtained by using the piston press (Δp = 1200 kPa): the dt/dV vs. V plots for experiments at pH 7, 11 and 13.3. The increase of the slope in the data set indicates the start of the expression phase.

The linear parts in the curves in Figs. 4 and 5 describe the period of cake formation, and the sharp increase in the slope in Fig. 5 indicates the start of the cake consolidation period. Eq. 8 was used to determine the average specific filtration resistance from the slope of the dt/dV vs. V curves during cake formation, which displayed a good linearity for all filtration experiments.
The average specific filtration resistance values for the experiments at different filtration pressures are depicted in Fig. 6a. The final average solidosities of the cakes (including expression for filtration at 1200 kPa), calculated on the basis of the cake dimensions (A x h) and the overall mass balance of the solids in the suspended and dissolved states, are presented in Fig. 6b.

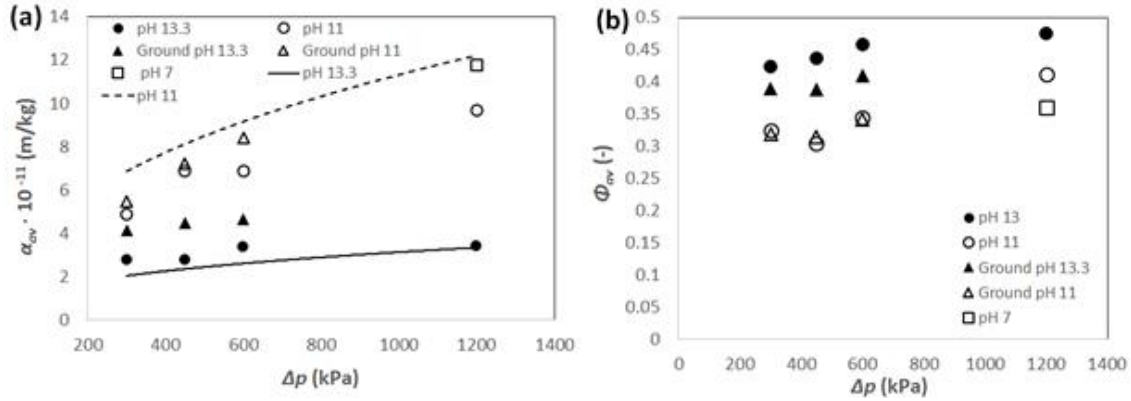

Figure 6. Average specific cake resistance, α_{av}, (a) and average solidosity, Φ_{av}, of the cake after filtration (and at 1200 kPa also expression) (b) at filtration pressure Δp for the original and ground bauxite residue slurries at pH 13.3, 11.0 and 7.0. The solid lines in Fig. 6a indicate the average specific filtration resistance calculated from local data by using Eq. (16) (based on the parameters presented in Table 4).

Regarding the average specific cake resistance, the cakes formed from the original bauxite residue slurry had the lowest values of α_{av} at all filtration pressures, while the reduction of the pH and grinding increased the filtration resistance of the formed filter cakes. The mechanical treatment had the largest effect at the 13.3 pH level, where also the greater effect on particle size distribution (Fig. 2a) could be observed. The pH reduction of the slurry was found to have a negative effect on filterability in all cases. Within the studied pH range, a large increase in filtration resistance took place between pH 13.3 and 11, for both ground and non-ground samples. A single experiment at pH 7 indicated a further, somewhat smaller increase in resistance for pH decrease down to pH 7. Also compressibility increased as the pH of the non-ground slurry was adjusted, as defined by Eq. (10): N was 0.36 at pH 13.3, while the slurry at pH 11 was considerably more compressible (N = 0.42).

The average cake solidosity became higher as the filtration pressure was increased. The effect of filtration pressure on the cake solidosity was, however, only moderate compared to the pH reductions, which resulted in a significant decrease in cake solidosity. The lower solidosity could be caused by a formation of larger agglomerates less prone to deformation under pressure, a phenomenon that has been illustrated earlier by Mattsson et al. [38] for a TiO_2 model system. The average specific cake resistance increased despite the decrease of cake solidosity, which suggests that the agglomerates formed had a looser structure and larger contact surface area with the filtrate compared to the particles/agglomerates at higher pH levels.

Additionally, the effect of grinding on Φ_{av} was negligible at pH 11, compared to that at pH 13, which is in agreement with the particle size data (Fig. 2a).

4.3 Local filtration properties

The local hydrostatic pressure profiles during the filtration experiments performed with the piston press for non-ground slurries at pH 13.3, 11.0 and 7.0 are presented in Fig. 7, for heights of 2-12 mm above the filter medium. As can be seen in Fig. 7, the absolute hydrostatic pressure (= Δp + 1 atm) at different heights in the cake is approximately 1300 kPa in the beginning of each experiment, i.e. corresponding to the applied filtration pressure. The pressure drop is steeper closer to the filter medium as the cake is formed, and slower as the distance from the filter medium increases. At the moment of time when the cake formation is completed, there is a contact between the piston and the top of the filter cake, the cake consolidation stage begins, and the liquid hydrostatic pressure deceases rapidly.

The local pressure profiles are in good accordance with the data presented in Fig. 5: the pressure profiles shown in Fig. 7 confirm that cake formation is a faster process when the pH is high. The sharp drop in local hydrostatic pressures at the end of the filtration period at pH 13.3 is also well visualized in Fig. 7, where the period between the point when expression begins to when the local hydrostatic pressure has dropped to levels close to ambient pressure is only about 200 s, compared to approximately 1500-2000 s for the slurries at pH 11 and 7, respectively. This change in the pressure profiles during the expression illustrates how the consolidation process is slower for the looser cake structures formed at a lower pH.

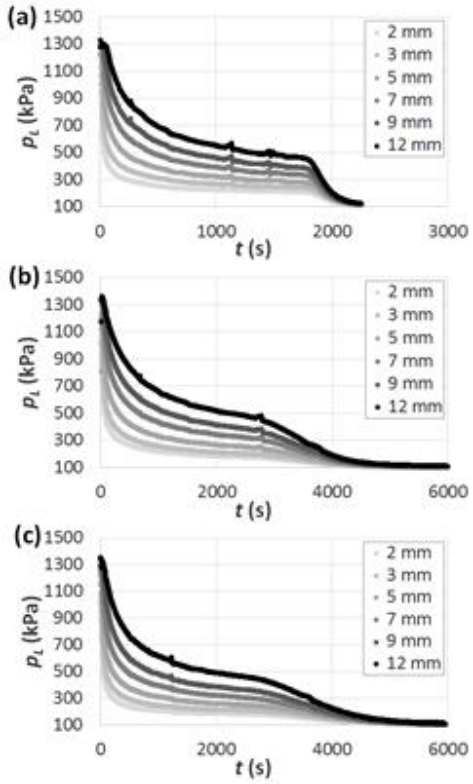

Figure 7. Local absolute hydrostatic pressure profiles in the filter cakes at different distances from the filter medium in the piston press: pH 13.3 (a), 11.0 (b) and 7.0 (c). Note the shorter time scale in Fig. 7a.

The hydrostatic pressure data, together with measured local solidosity and filtration flow, was also used for the estimation of the local specific cake resistances according to Eq. 13: the pressure gradient dp_L/dz needed was obtained from the hydrostatic pressure data at the positions of 9 and 12 mm, and solidosity was measured at the 12 mm position. The local specific filtration resistance and local solidosity are presented in Fig. 8a and 8b, respectively.

The semi-empirical constitutive relationships Eqs. (14) and (15) were fitted to the local specific filtration resistance and the local solidosity (Table 4, Fig. 8). To facilitate comparison between the individual filtration experiments, parameter p_0 was not fitted and was instead assigned a constant value (150 Pa). This restriction had a very limited influence on the quality of the fit.

Table 4. Parameters used for fitting Eqs. (14) and (15) to the experimental data.

Slurry pH	$\alpha_0 \cdot 10^{-10}$ (m/kg)	p_0 (Pa)	n (-)	Φ_0 (-)	β (-)
13.3	2.05	150	0.36	0.26	0.07
11.0	4.81	150	0.42	0.18	0.10
7.0	6.21	150	0.42	0.22	0.06

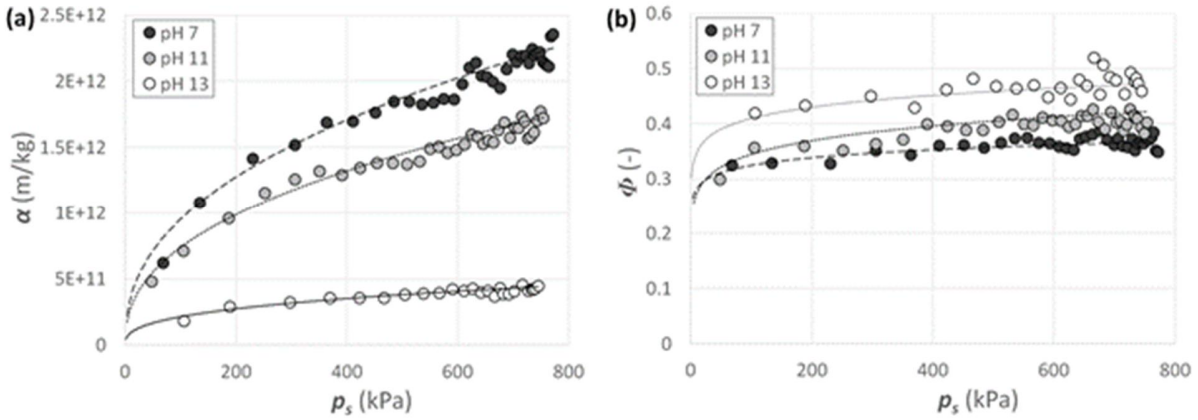

Figure 8. Local specific filtration resistance (a) and local solidosity (b), plotted against local solid compressive pressure for filtrations of slurries of varying levels of pH. The trendlines represent the values of α and Φ calculated from Eqs. (14) and (15) by using the parameters presented in Table 4.

The trends seen in the local data correspond well with the trends seen in the average data, Fig. 6, i.e. an increased specific filtration resistance, as well as an increased pressure dependence of the specific filtration resistance and a decreased solidosity at the lower pH levels. It should also be noted that one single experiment yielded local filtration data over a relative wide range of solid pressures. The most significant changes in the filtration behavior of the bauxite residue slurry took place between pH 13 and 11, while further reduction of the pH to 7 resulted in moderate changes only. This was also partly observable in the particle size data, where the effect of pH adjustment was clear above pH 11 but became less impactful as the pH was reduced further.

The empirical power-law models could be fitted to the experimental data with success (Fig. 8). The fitted parameters were used to estimate the average specific filtration by Eq. (16), where the pressure drop over the filter medium was neglected. The estimated filtration resistances are presented in Fig. 6a. At pH 13.3, a good agreement between the measured average filtration resistance and the resistances estimated from the local data can be observed. However, at pH 11, the estimations from local data result in a higher filtration resistance than the measured average filtration resistance. The reason for this difference is not fully understood, but it could be related to the increased compressibility of the filter cake at the lower pH 11 level. Further work is required to enable deeper understanding of this behavior.

5. Conclusions

The main objective of this experimental study was to investigate the average and local pressure filtration properties of bauxite residue slurries at the original and reduced pH levels. The slurries were characterized for particle size, chemical composition and rheology in order to interpret the changes taking place due to the pH adjustment.

It was shown that the filtration properties of the bauxite residue slurry were deteriorated by pH reduction, in spite of the increase of the particle or agglomerate size of the suspended solids. Adjustment of the slurry pH from the original pH of 13.3 to 11.0 increased the average filtration resistance (from $3.4 \cdot 10^{11}$ to $6.9 \cdot 10^{11}$ m/kg at a filtration pressure of 600 kPa), as well as the pressure dependence of the filtration resistance in the investigated filtration pressure range (300 kPa to 1200 kPa) significantly. The pH reduction also decreased the solidosity of the final filter cakes. Grinding the slurry material prior to filtration increased the filtration resistance and resulted in more porous cakes in experiments at slurry pH level of 13.3. However, grinding had a significantly lower impact at pH 11. These changes in filtration behavior were also observed in the local filtration properties. The local hydrostatic pressure measurements also indicated that the expression rates of the formed cakes were decreased for filter cakes formed from a slurry with a lower pH level (pH 11 and 7 compared to pH 13.3). The observations of filtration behavior and slurry properties suggest the formation of loose particle agglomerates in the slurry at lower pH levels, decreasing the solidosity of the formed cake and increasing cake resistance (due to increased surface area subjected to flow within the agglomerates).

References

[1] International Aluminium Institute, Bauxite residue management: best practice. (2015).

[2] K. Evans, The history, challenges, and new developments in the management and use of bauxite residue, J. Sustain. Metall. 2(4) (2016) 316–331.

[3] G. Power, M. Gräfe, C. Klauber, Bauxite residue issues: I. Current management, disposal and storage practices, Hydrometallurgy. 108 (2011) 33-45.

[4] W. Liang, S.J. Couperthwaite, G. Kaur, C. Yan, D.W. Johnstone, G.J. Millar, Effect of strong acids on red mud structural and fluoride adsorption properties, J. Colloid Interface Sci. 423 (2014) 158-165.

[5] C.R. Borra, B. Blanpain, Y. Pontikes, K. Binnemans, T. Van Gerven, Smelting of bauxite residue (red mud) in view of iron and selective rare earths recovery, J. Sustain. Metall. 2(1) (2015a) 28-37.

[6] M. Johnston, M.W. Clark, P. McMahon, N. Ward, Alkalinity conversion of bauxite refinery residues by neutralization, J. Hazard. Mater. 182 (2010) 710-715.

[7] V.A. Mymrin, A.J. Vazquez-Vaamonde, Red mud of aluminum production waste as basic component of new construction materials, Waste Manag. Res. 19 (2001) 465–469.

[8] Y. Zhao, J. Wang, Z. Luan, X. Peng, Z. Liang, L. Shi, Removal of phosphate from aqueous solution by red mud using a factorial design, J. Hazard. Mater. 165 (2009) 1193-1199.

[9] V.V. Grudic, S. Brasanac, V.L. Vukasinovic-Pesic, N.Z. Blagojevic, Sorption of cadmium from water using neutralized red mud and activated neutralized red mud, ARPN J. Eng. Appl. Sci. 8(11) (2013) 933-943.

[10] M. Ma, Y. Lu, R. Chen, L. Ma, Y. Wang, Hexavalent chromium removal from water using heat-acid activated red mud, Open J. Appl. Sci. 4 (2014) 275-284.

[11] B. Koumanova, M. Drame, M. Popangelova, Phosphate removal from aqueous solutions using red mud wasted in bauxite Bayer's process, Resour. Conserv. Recycl. 19 (1997) 11-20.

[12] J. Pera, R. Boumaza, J. Ambroise, Development of a pozzolanic pigment from red mud, Cement Concrete Res. 27 (1997) 1513-1522.

[13] Z. Liu, H. Li, Metallurgical process for valuable elements recovery from red mud—A review, Hydrometallurgy. 155 (2015) 29-43.

[14] I. Ghosh, S. Guha, R. Balasubramaniam, A.V.R. Kumar, Leaching of metals from fresh and sintered red mud, J. Hazard. Mater. 185 (2011) 662–668.

[15] Y. Huang, W. Chai, G. Han, W. Wang, S. Yang, J. Liu, A perspective of stepwise utilisation of Bayer red mud: Step two—Extracting and recovering Ti from Ti-enriched tailing with acid leaching and precipitate flotation, J. Hazard. Mater. 307 (2016) 318-327.

[16] P. Davris, E. Balomenos, D. Panias, I. Paspaliaris, Selective leaching of rare earth elements from bauxite residue (redmud), using a functionalized hydrophobic ionic liquid, Hydrometallurgy. 164 (2016) 125-135.

[17] C.R. Borra, Y. Pontikes, K. Binnemans, T. Van Gerven, Leaching of rare earths from bauxite residue (red mud), Miner. Eng. 76 (2015b) 20-27.

[18] Y. Liu, R. Naidu, Hidden values in bauxite residue (red mud): Recovery of metals, Waste Manag. 34 (2014) 2662-2673.

[19] M. Samouhos, M. Taxiarchou, P.E. Tsakiridis, K. Potidiaris, Greek "red mud" residue: A study of microwave reductive roasting followed by magnetic separation for a metallic iron recovery process, J. Hazard. Mater. 254-255 (2013) 193-205.

[20] S. Wang, H.M. Ang, M.O. Tade, Novel applications of red mud as coagulant, adsorbent and catalyst for environmentally benign processes, Chemosphere. 72 (2008) 1621-1635.

[21] M.W. Clark, M. Johnston, A.J. Reichelt-Brushett, Comparison of several different neutralisations to a bauxite refinery residue: Potential effectiveness environmental ameliorants, Appl. Geochem. 56 (2015) 1-10.

[22] K. Evans, Success and challenges in the management and use of bauxite residue. Bauxite Residue Valorisation and Best Practices, Leuven, Belgium, 5.-7. October 2015.

[23] S. Arslan, H. Ucbeyiay, B. Celikel, M. Baygul, S. Avcu, G.K. Demir, ETI Aluminium red mud characteristics and evaluation of dewatering performance. Bauxite Residue Valorisation and Best Practices Conference, Leuven, Belgium, 5.-7. October 2015.

[24] H. Sutar, S.C. Mishra, S.K. Sahoo, A.P. Chakraverty, H.S. Maharana, Progress of red mud utilization: An overview, Amer. Chem. Sci. J. 4(3) (2014) 255-279.

[25] X. Wang, Y. Zhang, F. Lv, Q. An, R. Lu, P. Hu, S. Jiang, Removal of alkali in the red mud by SO_2 and simulated flue gas under mild conditions, Environ. Prog. Sustain. Energy. 34(1) (2015) 81-87.

[26] P.L. Howe, M.W. Clark, A. Reichelt-Brushett, M. Johnston, Toxicity of raw and neutralized bauxite refinery residue liquors to the freshwater Cladoceran *Ceriodaphnia Dubia* and the marine Amphipod *Paracalliope Australis*, Environ. Toxicol. Chem. 30(12) (2011) 2817-2824.

[27] I. Smiciklas, S. Smiljanic, A. Peric-Grujic, M. Sljivic-Ivanovic, M. Mitric, D. Antonovic, Effect of acid treatment on red mud properties with implications on Ni(II) sorption and stability, Chem. Eng. J. 242 (2014) 27-35.

[28] M. Misik, I.T. Burke, M. Reismüller, C. Pichler, B. Rainer, K. Misikova, W.M. Mayes, S. Knasmueller, Red mud a byproduct of aluminum production contains soluble vanadium that causes genotoxic and cytotoxic effects in higher plants, Sci. Total Environ. 493 (2014) 883-890.

[29] A. Ghorbani, A. Fakhariyan, Recovery of Al_2O_3, Fe_2O_3 and TiO_2 from bauxite processing waste (red mud) by using combination of different acids, J. Basic Appl. Sci. Res. 3(1s) (2013) 187-191.

[30] M. Gräfe, G. Power, C. Klauber, Bauxite residue issues: III. Alkalinity and associated chemistry, Hydrometallurgy. 108 (2011) 60-79.

[31] L.J. Kirwan, A. Hartshorn, J.B. McMonagle, L. Fleming, D. Funnell, Chemistry of bauxite residue neutralisation and aspects to implementation, Int. J. Miner. Process. 119 (2013) 40-50.

[32] S. Khaitan, D.A. Dzombak, G.V. Lowry, Chemistry of acid neutralization capacity of bauxite residue, Environ. Eng. Sci. 26(5) (2009) 873-881.

[33] M.R. Thornber, D. Binet, Caustic soda adsorption on Bayer residues. In: Alumina, Worsley (Ed.), 5th International Alumina Quality Workshop. Bunbury, AQW Inc., 1981, pp. 498–507.

[34] B.F. Ruth, Studies in filtration III. Derivation of general filtration equations, Ind. Eng. Chem. 27(6) (1935) 708-723.

[35] H.P.G. Darcy, Les Fontaines Publiques de la Ville de Dijon. Victor Dalamont, Paris.
Dell, C. C. and Sinha, J., 1964. The mechanism of removal of water from flocculated clay sediments, Trans. Br. Ceram. Soc. 63 (1856) 603-614.

[36] R.G. Holdich, Solid-liquid separation equipment selection and modelling. Miner. Eng. 16 (2003) 75-83.

[37] T. Mattsson, J. Durruty, J. Wetterling, H. Theliander, The influence of ionic strength on the local filtration properties of titanium dioxide, Filtration. 15(1) (2015) 48-57.

[38] T. Mattsson, M. Sedin, H. Theliander, Zeta-potential and local filtration properties: Constitutive relationships for TiO_2 from experimental filtration measurements, Chem. Eng. Sci. 66 (2011) 4573-4581.

[39] T. Kinnarinen, R. Tuunila, M. Huhtanen, A. Häkkinen, P. Kejik, T. Sverak, Wet grinding of $CaCO_3$ with a stirred media mill: Influence of obtained particle size distributions on pressure filtration properties, Powder Technol. 273 (2015) 54-61.

[40] D. Chvedov, S. Ostap, T. Le, Surface properties of red mud particles from potentiometric titration, Colloids Surf. A. 182 (2001) 131–141.

[41] C. Johansson, H. Theliander, Measuring concentration and pressure profiles in deadend filtration, Filtration. 3(2) (2003) 114-120.

[42] L. Svarovsky, Solid-liquid separation, second ed., Butterworth & Co, Witham, Essex, 1981.

[43] I.T. Burke, C.L. Peacock, C.L. Lockwood, D.I. Stewart, R.J.G. Mortimer, M.B. Ward, P. Renforth, K. Gruiz, W.M. Mayes, Behavior of aluminum, arsenic, and vanadium during the neutralization of red mud leachate by HCl, gypsum, or seawater, Environ. Sci. Technol. 47 (2013) 6527-6535.

[44] Y. Liu, R. Naidu, H. Ming, Surface electrochemical properties of red mud (bauxite residue): zeta potential and surface charge density, J. Colloid Interface Sci. 394 (2013) 451–457.